

A Stepwise Regression and Statistical Downscaling Approach for Projecting Temperature Variations under Multiple RCP Scenarios

X. Huang¹, X. Zhou^{1*}, G. H. Huang¹, Y. P. Li¹, and Y. F. Li¹

¹State Key Joint Laboratory of Environmental Simulation and Pollution Control, School of Environment, Beijing Normal University, Beijing 100875, China

Received 15 December 2022; revised 20 January 2023; accepted 29 January 2023; published online 10 February 2023

ABSTRACT. With the rapid development of Central China, the temperature in this region is continuously increasing. Extreme weather events (e.g., high-temperature weather for many consecutive days) are becoming frequent. In order to provide future theoretical guidance on the direction of local development and the prevention of extreme natural disasters, the daily datasets of 12 meteorological stations in three provinces were collected. The corresponding predictors from 25 large-scale climatic factors were then screened using stepwise regression. A stepwise regression and statistical downscaling (SRSD) approach was developed to establish the statistical relationship. The future temperature results were projected by the weather generator, and the probability of extreme weather occurrence was analyzed by extreme values. The results indicate that future temperature in Central China shows an increasing trend from 2036 to 2065 and 2066 to 2095, with the representative concentration pathway 4.5 (RCP4.5) scenario showing a greater increase in temperature than the representative concentration pathway 8.5 (RCP8.5) scenario. Hunan Province has the largest temperature increase, followed by Hubei Province and Henan Province. The average annual duration of heat waves in Central China is 74.7 days.

Keywords: climate change scenarios, statistical downscaling, central china, stepwise regression and statistical downscaling

1. Introduction

According to the Blue Book on Climate Change in China (2020), the global average temperature in 2019 increased by about 1.1 °C compared with that before industrialization in the eighteenth century (National Climate Center, 2020). Since the 1980s, every decade has been warmer than the previous decade and warming trends have become apparent. This may be stemmed from the development of regional industry. With providing good economic development for the local area, the greenhouse gases generated in the process continuously sink into the atmosphere, which could increase the difficulty of global warming curbs and the probability of extreme climatic events. Therefore, the reasonable projection of future temperature changes has important practical significance for guiding the formulation of policies and measures to cope with climate change and disaster prediction.

In terms of statistical downscaling, there are also many studies and concerns about the simulation performance on air temperature. For example, Fan et al. (2013) compared the results predicted in the model with the measured data and found that the results were better in predicting the air temperature using statistical downscaling in China; the average maximum correlation coefficient of characterization error exceeded

or approached 0.90 in most areas. Among them, statistical downscaling model (SDSM) can combine multiple analysis methods and downscaling methods to simulate more accurate prediction results. Chen et al. (2012) introduced the SDSM statistical downscaling model in Jianghuai Basin based on the combination of multiple linear regression analysis and random weather generator for temperature estimation; the results showed that the extreme temperature data simulated by the statistical downscaling method were in a good agreement with observed temperature values. Liu et al. (2019) selected the SDSM model to study the trends and probabilities of future climate changes in the Ganjiang River Basin. Guo et al. (2012) used SDSM model to estimate the long-term temperature thermal effect and the resulting population death risk in Shanghai under scenarios A2 and B2; the results showed that the population death risk caused by temperature thermal effect in Shanghai will increase in the future, and the increase in the long-term death risk in the future is much higher than that in the mid-term future.

Central China includes Hubei, Hunan and Henan Provinces. From the actual situation in recent years, it can be seen that there is a relatively obvious increase in temperature, and the frequency, maximum and duration of high temperature events in summer have increased significantly. The Meteorological centers have issued hot-red-early warnings for many times, especially the surface temperature of some central cities is as high as 40 °C. For example, on August 2, 2021, the Meteorological Observatory of Wuhan issued a yellow-early warning signal of high temperature: it is expected that the maximum

*Corresponding author. Tel.: +86 15122694282.

E-mail address: zhou.xiong@outlook.com (X. Zhou).

temperature would reach more than 35 °C on most areas in our city and up to 37 °C locally in the next 3 days (National Early Warning Information Release Center, 2021). The factors contributing to these increases are multifaceted, but the changes and magnitude of trends thereafter should be sufficient to attract attention.

Based on the previous research, Coupled Model Intercomparison Project Phase 5 (CMIP5) has been fully proved to be highly suitable in China. The data is perfect and easy to obtain, which makes the research can be carried out more smoothly. In addition, there was often a lack of effective screening predictors in the previous research studies. Therefore, to effectively screen out predictors, it is feasible and innovative to introduce situational climate change in CMIP5 into the combination of SDSM and stepwise regression analysis to obtain more suitable temperature change estimation results in central China.

Therefore, the objective of this study is to develop a stepwise regression and statistical downscaling (SRSD) model for exploring the specific range of temperature increase in the context of greenhouse gas emissions, as well as the possibility of extreme weather. It is expected to provide theoretical support for the local government to enact appropriate policies and strategies under the local actual situation, comprehensive economic, environmental, demographic and other factors. The specific objectives are listed as follows: (1) Daily datasets of meteorological stations and corresponding climatic factors in National Centers for Environmental Prediction (NCEP) will be obtained; appropriate predictors from large-scale climatic factors will be identified by stepwise regression analysis. (2) The obtained data and predictors will be imported into SDSM model to establish statistical relationship; future temperature changes over central China will be developed through weather generator. (3) Probability analysis on the results of temperature changes will be performed; the trends in the frequency and duration of extreme weather events such as droughts will be analyzed. (4) Reasons for projection results in light of the regional characteristics will be explored; theoretical guiding opinions on the development strategies as well as disaster prevention and mitigation or response policies will be discussed.

2. Development of Stepwise Regression and Statistical Downscaling (SRSD) Model

In this study, we developed a stepwise regression and statistical downscaling (SRSD) model to achieve the purpose of analyzing temperature changes and the probability of extreme weather events. The flow chart is provided in Figure 1. Firstly, the stepwise regression analysis method is used to select the prediction factors. The basic idea of stepwise regression method is to select the most important variables from a large number of selectable variables, so as to establish a regression analysis prediction model between independent variables and dependent variables. The basic idea of stepwise regression is to introduce all independent variables one by one; the introduction condition is that the probability or frequency of F-test for the sum of squares of partial regression are significant and meet the set

values. At the same time, the old variables that have been introduced before are tested after each new variable is introduced; the old variables will be eliminated if the sum of squares of the flat regression is no longer significant after the new variable is introduced. By introducing new variables and removing the old variables, the regression equation is established between all independent variables and dependent variables.

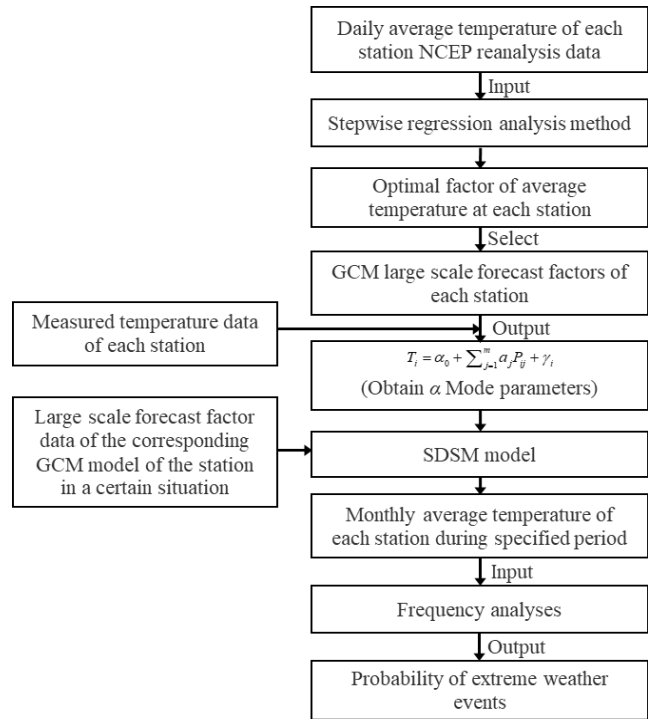


Figure 1. Technical flowchart.

In this study, the predictive factors most related to daily temperature at meteorological stations can be selected from 25 climatic factors by stepwise regression analysis. The regression equations are not required, but the significance of the impact of predictors on the measured data and the independence between predictors are ensured. Effective selection of predictive factors is a good premise for establishing statistical relationship and prediction model. There are some differences in the results of temperature changes predicted by different predictors, so it is necessary to select appropriate predictors under multivariate and multicollinearity conditions based on the stepwise regression analysis method.

The SDSM model is used to establish the statistical relationship between large-scale climate data and measured data. The large-scale GCM models under different CMIP5 scenarios will be inputted into SDSM to obtain temperature changes in central China. SDSM merges the idea of random weather generators in a variety of traditional multiple regression methods (Wilby et al., 1999). This combination helps to better function the two methods. Specifically, multiple regression methods will make the interannual variability estimate too low; however, random weather generators can overcome this weakness by relying

on their random simulation technique, which could make the variance of daily data sequences closer to the actual observed value (Chen et al., 2012).

Multiple regression method refers to the regression method of studying one dependent variable and two or more independent variables. Linear or nonlinear quantitative relationships between multiple variables or between multiple independent variables and dependent variables can be established to reflect the law that the number of a phenomenon or thing is affected by the change of the number of multiple phenomena or things, which thus can produce the corresponding change. Therefore, multiple regression is a regression model between a dependent variable (predicted object temperature) and multiple independent variables (predictors). For multiple linear regression, let x_1, x_2, \dots, x_m be m independent variables that can be accurately measured or controlled. If y is linearly related to m independent variables (i.e., x_1, x_2, \dots, x_m) data for group t , the relationship between dependent variable y_i and independent variables (i.e., $x_{i1}, x_{i2}, \dots, x_{im}$) will be obtained after t trials, which can formulated as follows:

$$\begin{aligned} y_1 &= a_0 + a_1x_{11} + a_2x_{12} + \dots + a_mx_{1m} + \beta_1 \\ y_2 &= a_0 + a_1x_{21} + a_2x_{22} + \dots + a_mx_{2m} + \beta_1 \\ &\dots\dots \\ y_t &= a_0 + a_1x_{t1} + a_2x_{t2} + \dots + a_mx_{tm} + \beta_1 \end{aligned} \quad (1)$$

where $i = 1, 2, \dots, t$; $a_0, a_1, a_2, \dots, a_m$ are $m + 1$ coefficients to be estimated; β_i denotes the effect of random factors on y_i in the i^{th} trial. For simplicity, this t -equation is represented as a matrix form:

$$Y = XA + B \quad (2)$$

where $Y = (y_1, y_2, \dots, y_t)$, $A = (a_0, a_1, a_2, \dots, a_m)$ and $B = (\beta_1, \beta_2, \dots, \beta_t)$. The formula above is the mathematical model of m -element linear regression (Fu et al., 2003).

Random weather generators are a series of statistical models, which can construct climatic elements through stochastic simulation processes. They can be simply regarded as complex random number generators. The weather generator can obtain a complete statistical relationship model by directly fitting the actual observed values of climatic factors. The model is then used to simulate time series of climatic variables randomly. One of its advantages is that it cannot only generate the mean value of climate variables, but also adjust climate variability, resulting in an arbitrary length of time series to meet requirements (Wu and Wang, 1998). The basic principle can be summarized as the following formula based on the above:

$$T_i = \alpha_0 + \sum_{j=1}^m \alpha_j P_{ij} + \gamma_i \quad (3)$$

where T_i is the temperature variable (e.g., daily average); P_{ij} is a large-scale predictor; m is the number of predictors; α is the mode parameter; γ_i is the mode error.

After obtaining the future temperature change data, the

probability of extreme weather events in the future based on the specific trend of the data can be calculated. Because extreme events are small probability events, they are reflected in temperature projections that their values deviate from the extreme values at both ends of the normal value. Extreme weather events are extremely damaging to the economy of the region as well as to the safety of the people, so it is necessary to analyze and prevent them in advance. In general, the exact distribution of extreme values is difficult to determine, and the gradual distribution of extreme values is mainly investigated (Wang et al., 2006; Li, 2007; Wu, 2009; Gu et al., 2019). The main extreme value distributions can be summarized as: Let X_1, X_2, \dots, X_n be independent and identically distributed random variables with a distribution function $F(X)$ such that $Y_n = \max(X_1, X_2, \dots, X_n)$. The distribution function of Y_n is $T(X) = F_n(X)$. If there is $a_n > 0$ and $b_n (n \rightarrow \infty)$, the probability $T(X) = Pr\{(Y_n - b_n) / a_n \leq X\}$ holds, $T(X)$ is belong to three distributions (Shi, 2006; Zhang et al., 2021).

Gumbel Extreme Value Distribution:

$$T(X) = \exp[-\exp(-x)] \quad (4)$$

Frechet Extreme Value Distribution:

$$T(X) = \begin{cases} 0, & x \leq 0 \\ \exp(-x^\beta), & x > 0 \end{cases} \quad (5)$$

Weibull Extreme Value Distribution:

$$T(X) = \begin{cases} \exp[-(-x)^\beta], & x \leq 0 \\ 1, & x > 0 \end{cases} \quad (6)$$

where β is the distribution parameter in Equations (5) and (6).

3. Overview of the Study Area

Central China (Figure 2), as one of the seven geographical subdivisions of China, includes the provinces of Henan, Hubei and Hunan. It is located in central China and mainly covers the middle and lower reaches of the Yellow River as well as the middle reaches of the Yangtze River. In the hinterland of China, it is bordered by five geographical subdivisions: North China, East China, South China, Northwest China and Southwest China. It has many national trunk lines and is a key road to connect all parts of the country. The topography and landforms of central China are very diverse, mainly including mountains, plains, hills, basins, etc. Therefore, many microclimatic characteristics have emerged, which are still temperate monsoon climates and subtropical monsoon climates. However, the temperature changes in different regions are not stable due to a variety of factors.

The climate of central China is divided into Qinling Mountains and Huaihe River. The south of Huaihe River is subtropical monsoon climate, and the north is temperate monsoon climate. Some scholars have studied temperature changes based

on the historical phenological records of the past 150 years in central China. The results show that temperature changes in central China have been obviously characterized by interannual to interdecadal fluctuations since the 1950s; however, the main cycle of change before the 1920s is about twelve to fourteen years. The economy of central China has been developed rapidly after the 1990s, when the subsequent warming trend and range significantly exceed the previous interdecadal fluctuation level. At the end of the last century, the temperature has increased significantly compared with the same cycle in the middle of the last century (Zheng et al., 2015).

Based on the principle of spatial uniform distribution, four meteorological stations were selected in each province. Their location distributions are shown in Figure 2. In this study, daily mean temperature was used from 1980 to 2010 at 12 weather stations, which are distributed evenly in the provinces of Henan, Hubei and Hunan. The data were obtained from the National Oceanic and Atmospheric Administration (NOAA) and National Centers for Environmental Information (NCEI). The corresponding year and region of NCEP datasets came from the physical science laboratory (PSL) with a horizontal resolution of $1.5^\circ \times 1.5^\circ$. The climatic factors to be screened were included 25 factors such as geopotential height, relative humidity, east wind, and north wind in different pressure layers. The global climate model was The Canadian Earth System Model version 2 (CanESM2) with a horizontal resolution of $2^\circ \times 2.5^\circ$. The scenarios are RCP4.5 and RCP8.5, which derived from CMIP5 of World Climate Research Program (WCRP). The SDSM model used is obtained in <https://sdsml.org.uk/sdsmlmain.html>, and Version is 5.3 more stable.

4. Model Evaluation

The observed data and the NCEP predictor from 1980 to 1995 for the calibration model are shown in Table 1. It shows the range of results for R^2 , Standard Error (SE), and Debin Watson for each month at each meteorological station. The R^2 values shows that the model can be sufficient used to project future monthly temperatures. In addition, the calibration model for each site meets the requirements of Debin Watson, most of which are close to 2. Moreover, the SE values are between 2.5 and 5.5, which shows that the relative deviation between the simulated values and observed values is small.

In general, the four stations in Henan Province have better R^2 , with SE values below 4.5. Although the initial Debin Watson value is low, it is within the reasonable error range. It may have a certain relationship with the high temperature in summer. Model calibration fitting is good in each month in Hubei province. The low values of Debin Watson in Jingzhou indicate that there is a positive correlation among the predictors. R^2 is too low in several individual months. Compared with Henan Province, the SE value of Hubei Province is a little higher, that is, simulated values are slightly different from observed values. The calibration results of four meteorological stations in Hunan Province are better than those in Henan Province. The Debin Watson and R^2 of each station are relatively concentrated in Hunan Province.

In addition, there are some differences in the prediction factors selected from each station, which indicates that different regions are affected by different climatic factors. The cali-

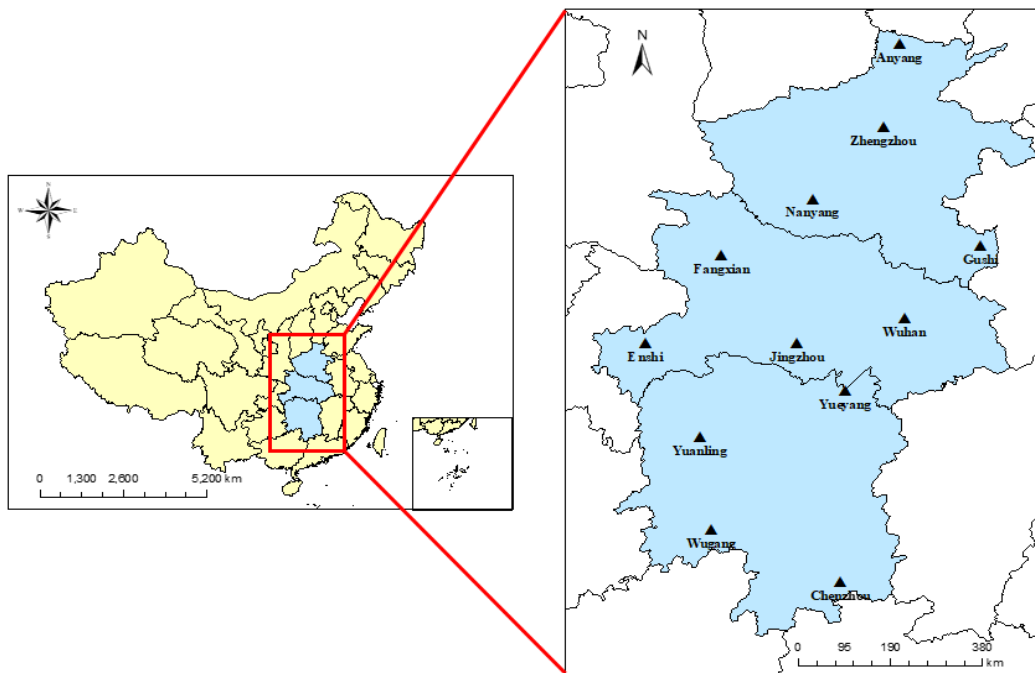


Figure 2. Geographical location map of central China and selected meteorological stations (meteorological stations including Zhengzhou, Anyang, Nanyang and Gushi in Henan Province; Wuhan, Enshi, Fangxian and Jingzhou in Hubei Province; Nanyueyang, Yuanling, Wugang and Chenzhou in Hubei Province).

Table 1. Calibration Result of Meteorological Station Model

Site Name	Durbin-Watson	R^2	SE
Zhengzhou	1.870 ~ 2.179	0.487 ~ 0.753	2.706 ~ 4.482
Anyang	1.914 ~ 2.278	0.494 ~ 0.735	2.708 ~ 4.334
Nanyang	1.823 ~ 2.171	0.538 ~ 0.745	2.550 ~ 4.118
Gushi	1.689 ~ 2.126	0.553 ~ 0.768	2.610 ~ 4.294
Wuhan	1.859 ~ 2.039	0.268 ~ 0.591	3.117 ~ 5.462
Enshi	1.850 ~ 2.051	0.240 ~ 0.692	3.173 ~ 5.192
Fangxian	1.742 ~ 2.043	0.379 ~ 0.706	2.980 ~ 4.713
Jingzhou	1.597 ~ 1.982	0.364 ~ 0.669	2.973 ~ 5.388
Yueyang	1.610 ~ 2.080	0.429 ~ 0.685	2.814 ~ 4.777
Yuanling	1.608 ~ 2.090	0.425 ~ 0.685	2.872 ~ 4.812
Wugang	1.740 ~ 2.085	0.349 ~ 0.695	2.989 ~ 4.764
Chenzhou	1.834 ~ 2.092	0.242 ~ 0.691	3.155 ~ 5.200

Table 2. Standard Deviation Table for Comparison of Projection and NCEP Observed Results by Site

Site Name	Standard Deviation (°C)	R^2
Zhengzhou Henan	0.257	0.9312
Anyang Henan	0.251	0.9337
Nanyang Henan	0.310	0.9453
Gushi Henan	0.321	0.9500
Wuhan Hubei	0.322	0.9542
Enshi Hubei	0.265	0.9379
Fangxian Hubei	0.277	0.9385
Jingzhou Hubei	0.349	0.9412
Yueyang Hunan	0.395	0.9535
Yuanling Hunan	0.298	0.9352
Wugang Hunan	0.405	0.9307
Chenzhou Hunan	0.521	0.9340

Table 3. Projection Standard Deviation of Temperature for Each Site under CanESM2 Model

Site Name	Standard Deviation (°C)	R^2
Zhengzhou Henan	0.221	0.9329
Anyang Henan	0.217	0.9343
Nanyang Henan	0.261	0.9480
Gushi Henan	0.270	0.9512
Wuhan Hubei	0.282	0.9543
Enshi Hubei	0.227	0.9370
Fangxian Hubei	0.242	0.9394
Jingzhou Hubei	0.300	0.9387
Yueyang Hunan	0.338	0.9538
Yuanling Hunan	0.255	0.9344
Wugang Hunan	0.350	0.9301
Chenzhou Hunan	0.452	0.9351

brated model is used to simulate the monthly mean temperatures from 1996 to 2005. The results are compared with the NCEP datasets. The fitted standard deviations for each site are shown in Table 1. The simulated monthly mean temperature is compared to the NCEP temperature to verify the degree of suitability of this NCEP reanalysis dataset in this model. This is the initial step in model input and the basis following the screening

of predictors. As shown in Table 2, the simulation results of the developed model are relatively good, with annual standard deviations of less than 0.55 °C and R^2 greater than 0.90, demonstrating that it is appropriate to select the input model for this dataset.

The calibrated model is then used to load the CanESM2 model and predict the monthly mean temperature from 1981 to 2010. The obtained standard deviation values and R^2 of the monthly mean temperature at each station under this model during the simulation are shown in Table 3. The selection of CanESM2 mode and the selection of predictors for each site are appropriate, with standard deviations less than 0.50 °C and R^2 greater than 0.90. Therefore, from the above, it is feasible to input the NCEP reanalysis dataset and load the CanESM2 mode for the next step for model simulation under RCP4.5 and RCP8.5 in CMIP5. The prediction results are more credible.

5. Projection for Temperature Variations

The results of monthly mean temperature changes at different time periods (i.e., 1981 ~ 1995, 1996 ~ 2005, 2036 ~ 2065, and 2066 ~ 2095) obtained from 12 weather stations under two emission scenarios (i.e., RCP4.5 and RCP8.5) will be analyzed. First, the temperature trend chart of four meteorological stations in Henan Province is shown in Figure 3. According to Figure 3, temperature change trends of four stations in Henan Province are consistent, showing an increasing trend in spring and summer. However, the curve is relatively compact, that is, the temperature change is small. The temperature change of Nanyang station in Henan province in May and October is more obvious under different scenarios. This indicates that the greenhouse gas emissions have a greater impact on the temperature of this region in these two months. Temperature in May and November at Gushi station in Henan are more significantly increased, showing a more obvious breakpoint change. These increases show that the temperature in this area is more sensitive to greenhouse gas emissions.

The temperature trend change chart corresponding to the four weather stations in Hubei Province is shown in Figure 4. It can be seen from Figure 8 that the variation trend of Wuhan station is similar to those of the four stations in Henan Province. This may be due to the fact that all of them are in the plain area and have similar latitude, which makes the predictor have certain similarity in principle. Similarly, the most obvious change at Wuhan station was in November. The variation trends of Fangxian station and Wuhan station in Hubei province are similar. The temperature increases in May are more obvious than other months. Its autumn and winter seasons show a continuous temperature increase, which means that the impact of greenhouse gas emissions on this area is continuous in time. The temperature increases in different months, while the impact range is smaller in summer.

The change trends of Enshi station in Hubei province and Jingzhou station in Hubei province are similar, but slightly different from Wuhan station and Fangxian station. It can be seen that in addition to the slight increase in May and the continuous

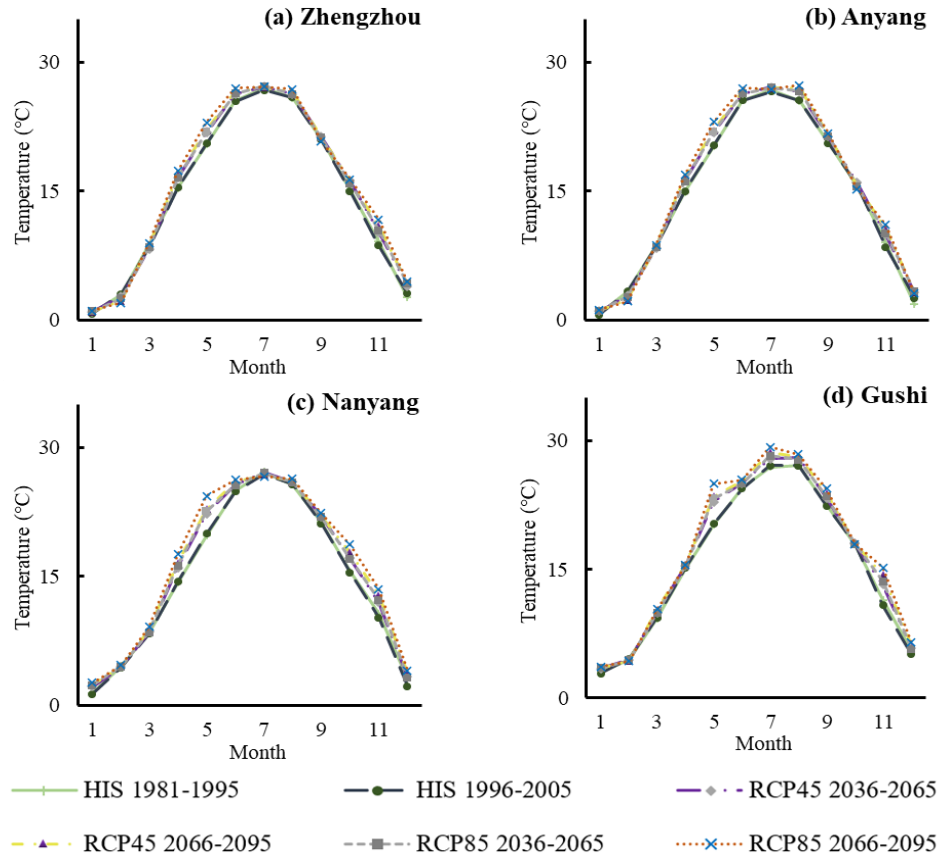


Figure 3. Trends of monthly mean temperature of four meteorological stations in Henan Province over six time periods under two scenarios; (a) ~ (d) is the Zhengzhou, Anyang, Nanyang, and Gushi site, respectively.

increase in autumn and winter, the temperature of these two stations decrease to a certain extent in July. From the point of view of greenhouse gas emission, its influence on the temperature of this area still exists and is continuous in time. However, due to the topography of mountainous hills and flourishing vegetation, it has a better cooling effect in the summer. In addition, its industrialization and urbanization degree are much lower than those in Wuhan, which may be an important reason for decreasing temperature in summer.

The temperature variation trend chart of four weather stations in Hunan Province is shown in Figure 5. According to Figure 5, the temperature change of four weather stations in Hunan Province is more obvious than those in Henan Province. The change trend of Yueyang station is similar to that of Chenzhou station in Hunan province. The main increase months are November and May, and the decrease range is not obvious in July. However, the Yueyang station is continued to warm up in winter, while Chenzhou station is continued to warm up in spring. The Yuanling station is mainly showed a significant warming trend in April and May. The overall warming trend of Wugang in Hunan Province is relatively obvious, but the temperature increase in May shows an explosive growth. On the basis of excluding errors or model simulation errors, the analysis of this result may be because the latitude of this station is low on the one hand; on the other hand, it can be seen that the greenhouse

gas emissions have a more obvious effect on the temperature increase of each station in May.

In general, it can be seen from Figure 3 to Figure 5 that the temperature changes of 12 stations showed a significant increasing trend in summer at different time periods, but a slight decreasing trend in winter. In summer, the temperature of each site is increased under the RCP4.5 scenario, and the increase is higher from 2066 to 2095 than from 2036 to 2065; The temperature is also showed an increasing trend under the RCP8.5 scenario. The increase from 2036 to 2065 under this scenario is basically equivalent to the increase from 2066 to 2095 under the RCP4.5 scenario, while the increase is greater from 2066 to 2095 under RCP8.5. In winter, the decreasing trend of temperature is the same as the increasing trend in summer, that is, it shows the decreasing results of RCP4.5 from 2036 to 2065, RCP8.5 from 2036 to 2065, RCP4.5 from 2066 to 2095, and RCP8.5 from 2066 to 2095.

The projection temperatures obtained from the two scenarios of RCP4.5 and RCP8.5 for the next two time periods of 2036 to 2065 and 2066 to 2095 are subtracted from the simulated temperatures obtained from the model for the corresponding stations from 1981 to 1995 in order to obtain increases and decreases of the four stations in each province at different times and months under the two scenarios. Figure 6 shows monthly mean temperature changes of four stations in Henan Province

from 1981 to 1995. After analyzing the increasing trend, it can be seen that the average temperature in February at all four stations has decreased to some extent. Specifically, the winter temperature is lower, which also means that the duration of extreme events (i.e., cold wave) may increase. In particular, the temperature changes in Zhengzhou and Anyang in Henan Province generally show a smaller increase, while the winter decrease are more obvious. However, the Nanyang and Gushi stations increase more significantly in the spring and winter. This may be more related to latitudinal location. The relatively high latitudes of Zhengzhou and Anyang make them receive relatively less light and lower temperature. Nanyang and Gushi stations not only receive more heat, but also are affected by the insulation effect of greenhouse gases.

The histogram of monthly average temperature increases and decreases at each site in Hubei Province is shown in Figure 7. According to Figure 7, Changes in Wuhan are similar to those in Hunan Province, showing a cooling in February and July. In addition to that, the cooling in July is particularly obvious in Enshi, Hubei Province and Jingzhou. The winter in Fangxian County still shows a warming trend, but the July and August in summer slightly cool down. Figure 8 shows temperature changes at each station in Hunan Province. Overall, the average monthly temperature of each station in Hunan Province generally shows

a warming trend, and the range of changes is more obvious, especially in April, May, and June of spring. Temperature in autumn is also slightly warmed, while the corresponding cooling in winter is not obvious. Yuanling shows a trend of warming throughout the year. Due to the large warming values in May, the longitudinal coordinate axis of the histogram of Wugang in Hunan Province has been adjusted to some extent. In addition, it also shows an obvious warming tendency in spring and autumn. However, the warming in summer is not significant, and there is no cooling trend in winter.

From Figures 6 to 8, the 12 weather stations show increases in temperature for most months, while some of them show a relative decrease in temperature in February, March, and July. The magnitude of temperature changes increases with time periods and GHG emissions, which is consistent with the trend chart above. Among them, under the RCP4.5 scenario, Henan Province increases by a maximum of 3.31 °C in May of Gushi, followed by 2.88 °C in November of Gushi. Henan Province decreases by a maximum of 0.96 °C in February of Anyang; Hubei Province increases by a maximum of 4.12 °C in November of Jingzhou and decreases by a maximum of 1.64 °C in July of Jingzhou; Hunan Province increases by a maximum of 4.14 °C in November of Yueyang and a maximum of 0.30 °C in February of Chenzhou. The general trend of temperature reduction

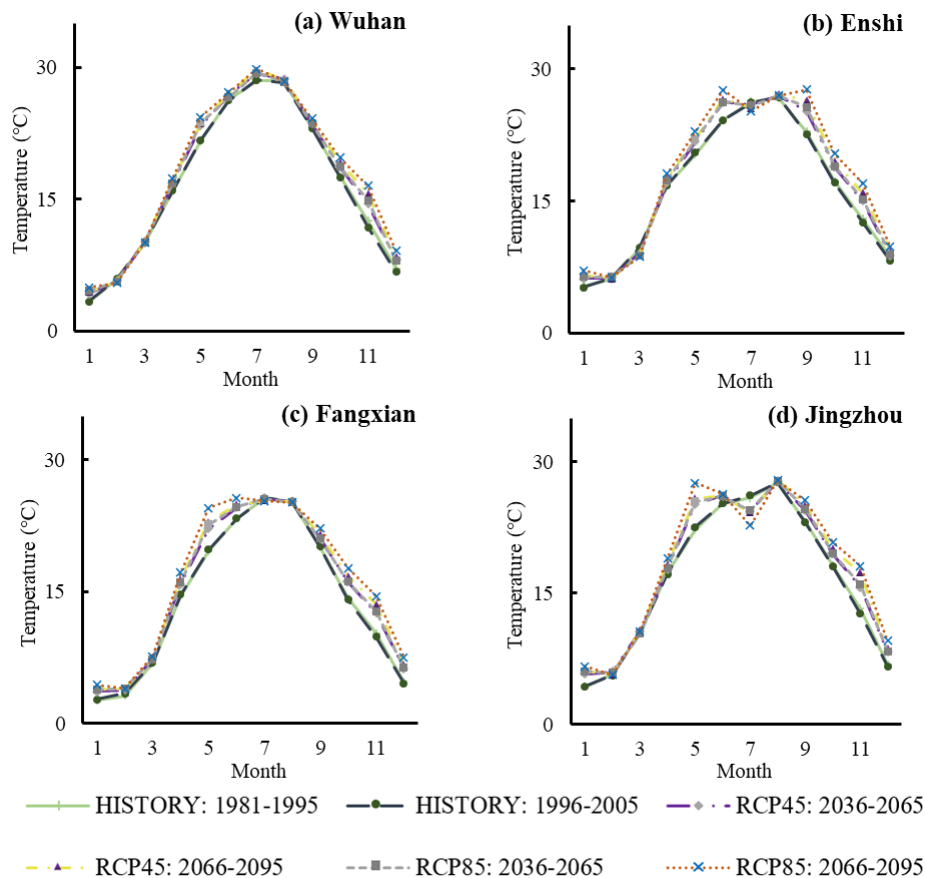


Figure 4. Trends of monthly mean temperature of four meteorological stations in Hubei Province over six time periods under two scenarios; (a) ~ (d) is the Wuhan, Enshi, Fangxian, and Jingzhou site, respectively.

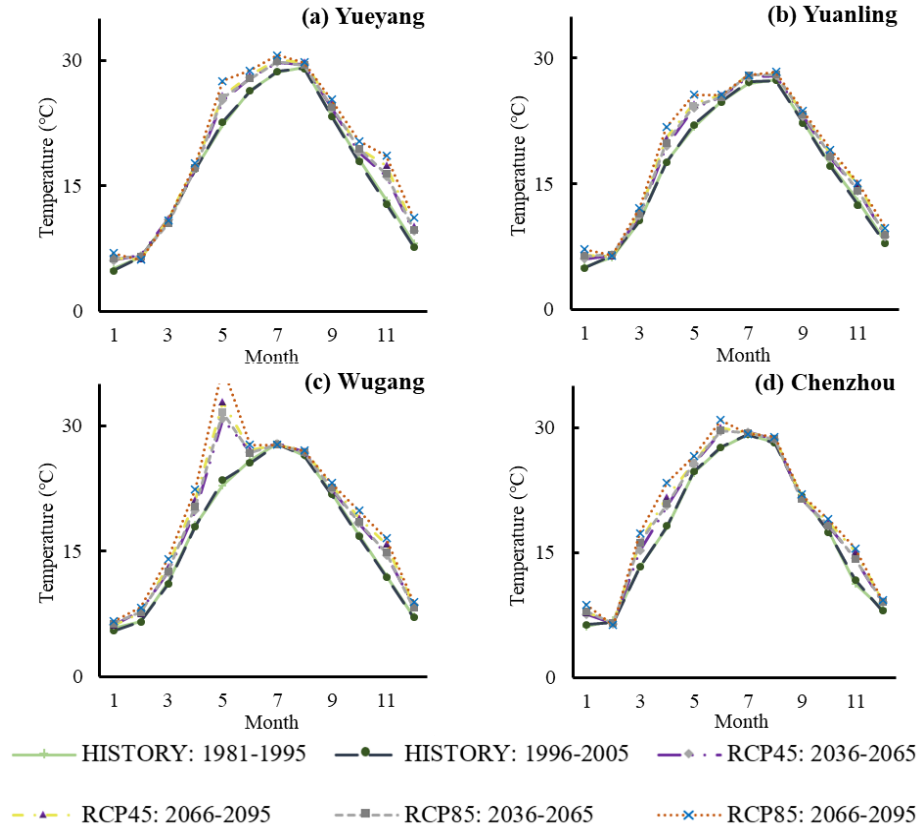


Figure 5. Trends of monthly mean temperature of four meteorological stations in Hunan Province over six time periods under two scenarios; (a) ~ (d) is the Yueyang, Yuanling, Wugang, and Chenzhou site, respectively.

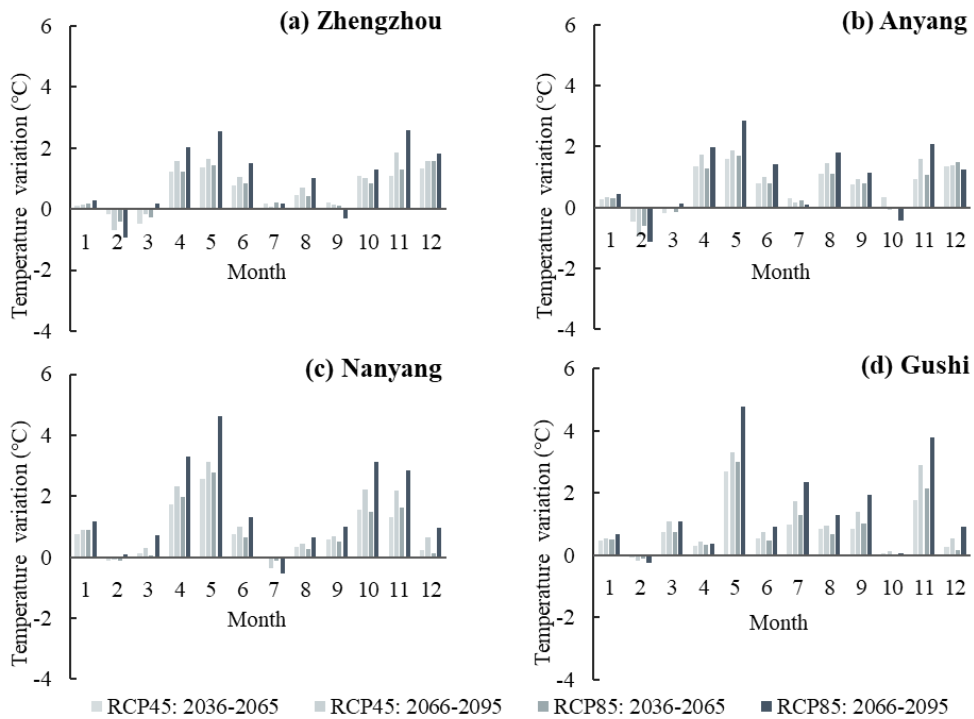


Figure 6. Increase and decrease of monthly mean temperature change of four meteorological stations in Henan Province in four time periods under two scenarios; (a) ~ (d) is the Zhengzhou, Anyang, Nanyang, and Gushi site, respectively.

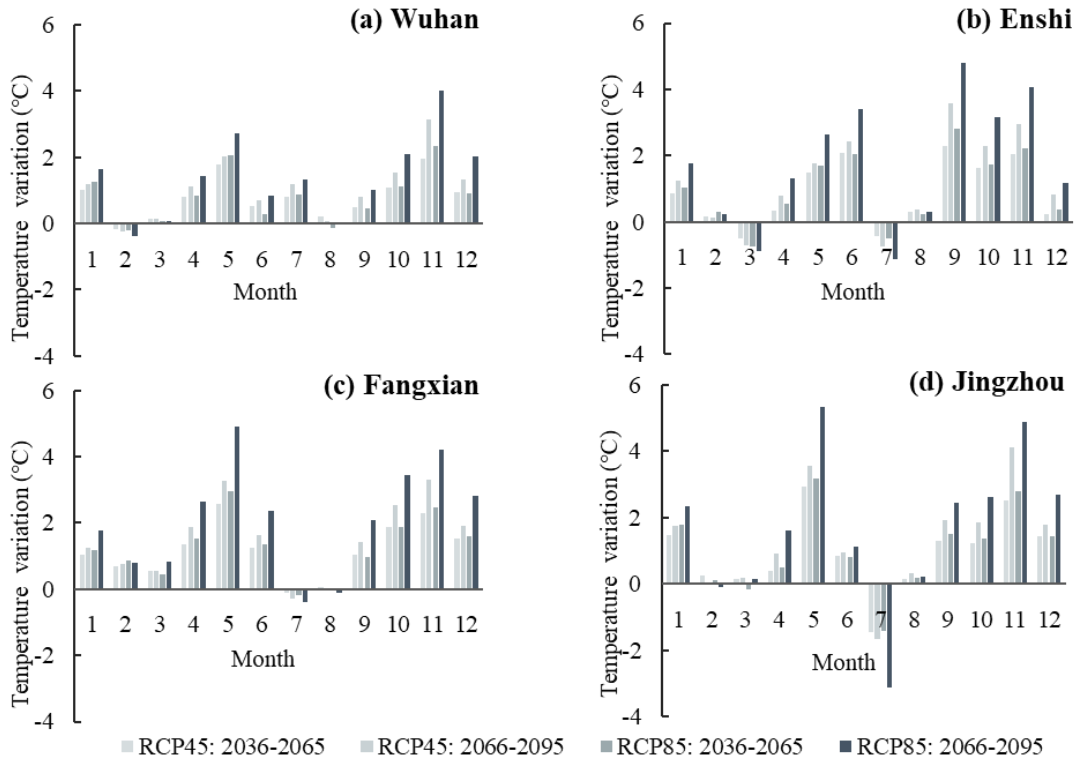


Figure 7. Increase and decrease of monthly mean temperature change of four meteorological stations in Hubei Province in four time periods under two scenarios; (a) ~ (d) is the Wuhan, Enshi, Fangxian, and Jingzhou site, respectively.

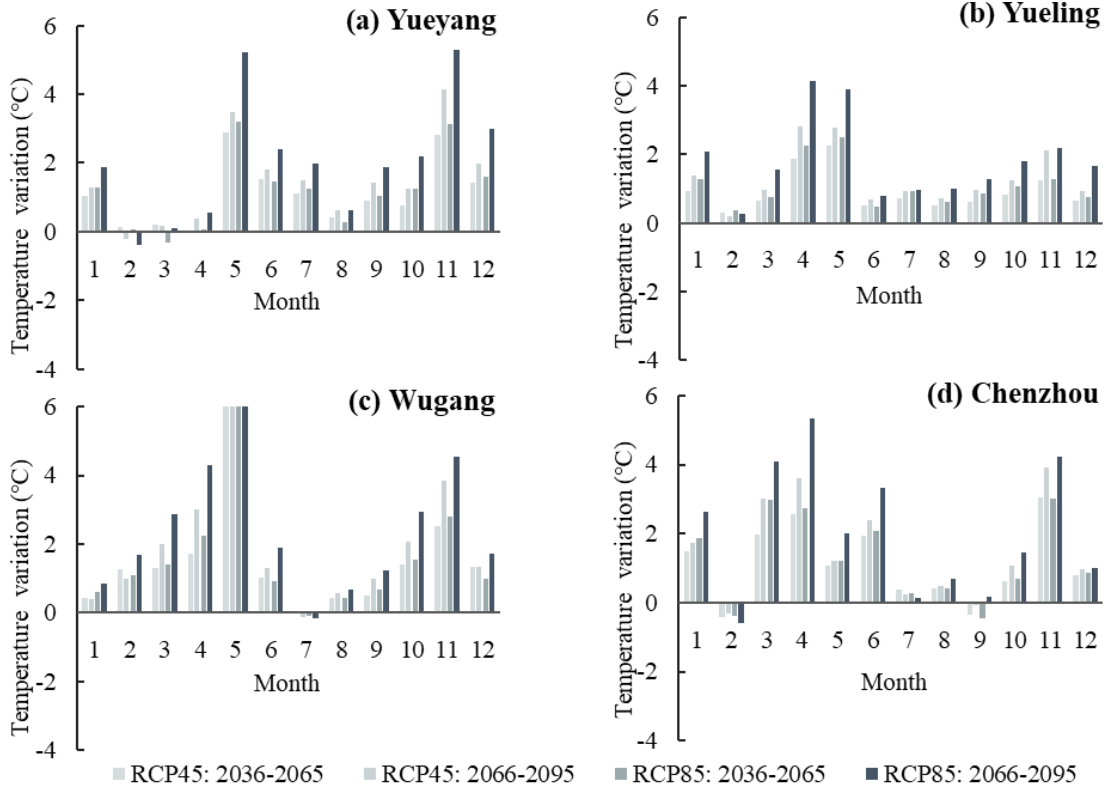


Figure 8. Increase and decrease of monthly mean temperature change of four meteorological stations in Hunan Province in four time periods under two scenarios; (a) ~ (d) is the Yueyang, Yuanling, Wugang, and Chenzhou site, respectively.

was not significant.

Under the RCP8.5 scenario, the largest increase in Henan Province is 4.76 °C in May Gushi, followed by 3.77 °C in November Gushi; The largest increase in Hubei Province is 4.87 °C in November Jingzhou, with the largest decrease of 3.14 °C in July Jingzhou; The largest increase in Hunan Province is 5.34 °C in April Chenzhou, with the largest decrease of 0.59 °C in February Chenzhou. In addition, the increase in May at Wugang site in Hunan is significant and much higher than that at other sites during the same period, with an increase as high as 14.17 °C under the RCP8.5 scenario. Yuanling station in Hunan Province shows a trend of increasing temperature throughout the year, even in winter.

After averaging the monthly average temperature changes in the two time periods under RCP4.5 and RCP8.5, the average increase values per month are presented in Figure 9. The data presented in this figure are the results obtained by arithmetic mean of changes in mean temperature for each month at each station in Figures 6 to 8. This process loses some of the lower winter temperature values, but the final results reflect the trend of RCP4.5 and RCP8.5 for future temperature increases. As can be seen from Figure 9, overall future temperatures tend to increase with enlarged greenhouse gas emissions. The increases under the RCP8.5 scenario are more significant than those under RCP4.5 scenario in the same period. It is indicated that greenhouse gas emission concentration has a greater impact on temperature than time periods.

In addition, the range of temperature increase is similar in the same latitude area, such as Wuhan, Enshi, Jingzhou and Yueyang stations. Secondly, it can be concluded that the lower the latitude, the greater the temperature increase; The largest of increase is the Wugang station in Hunan province. This suggests that the low latitude region not only has a higher base temperature, but also can maintain more heat under the addition of greenhouse gases, making the regional temperature remain high.

First, the temperature estimation results of the three provinces under the time change increased slightly from 2036 to 2065, increased more significantly from 2066 to 2095, and increased more significantly than the previous time period. This should be due to the gradual accumulation of greenhouse gases over time. On the other hand, the temperature change of three provinces under RCP8.5 scenario also showed a significant upward trend. The increase from 2036 to 2065 was slightly lower than that from 2066 to 2095 under the RCP4.5 scenario, while the increase from 2066 to 2095 increased further, basically reaching a 60-year time increase equivalent to the temperature change value of the 1.5-century time span from the middle of the nineteenth century to the beginning of the twenty-first century. Thus, the temperature rise was more pronounced in the RCP8.5 scenario compared to the RCP4.5 scenario, which demonstrates that more GHG emissions have a significant effect on the trend of temperature rise and are positively correlated.

From the changes in each month, it can be found that the increase in summer is not obvious or even shows a decrease phenomenon. It is indicated that the high temperature is also a certain upper limit. According to the estimation results within

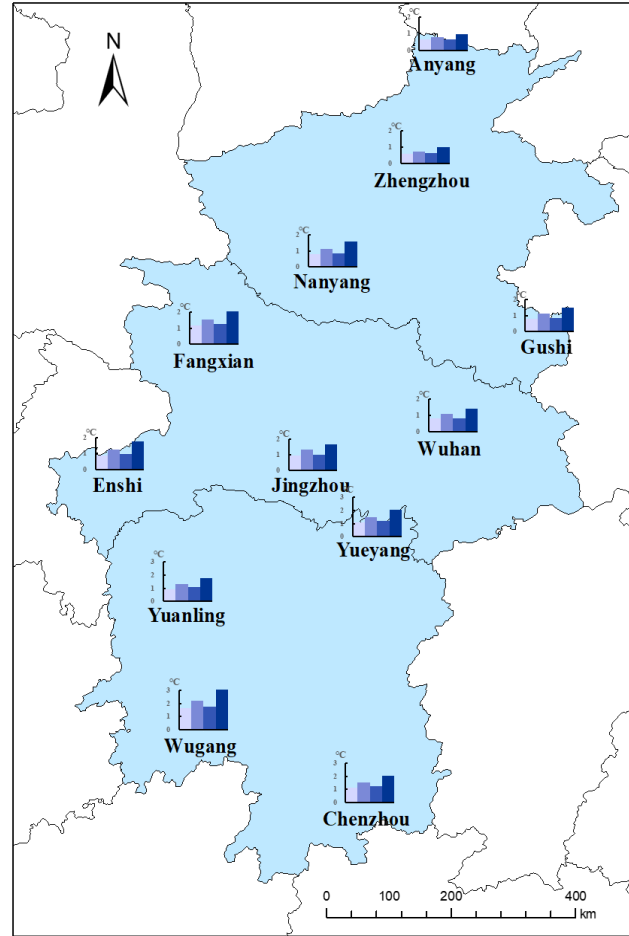


Figure 9. Average monthly increase and decrease temperature plots for the two time periods under RCP4.5 and RCP8.5 scenarios.

one hundred years, the monthly average temperature of each province is the highest value. In contrast, the increase is significant in March, April and May in spring and autumn, which indicates that the effect of greenhouse gas emissions on temperature rise is not completely reflected in the highest temperature. In addition, more of them are acted in the state of high temperature for a long time. In this respect, extreme value analysis of the results is highly desirable.

Among the three provinces, Hunan Province has the largest increase, which suggests that latitude is also crucial for the effect of temperature. The temperature change in Henan Province is not only reflected in the increase in summer, but also reflected in the decrease in winter. This may be related to the population growth and economic development of Henan Province. More population accommodation will lead to more economic development needs and environmental bearing damages. Because there are many rivers and lakes in Hubei province, the relative humidity in the atmosphere and the water circulation promotes the temperature change to maintain a relatively stable state. On the other hand, the topography in southwest China is mainly mountainous and hilly. Specifically, the topography changes greatly,

and the temperature changes linearly with altitude. Therefore, the changes of Enshi station in Hubei province are slightly different from those in the other three stations in each month.

The maximum increase in Hubei Province under the RCP4.5 scenario is similar to that in Hunan Province. The maximum increase in Hubei Province under the RCP8.5 scenario is similar to that in Henan Province. In other words, Henan Province and Hunan Province are more sensitive to the impact of scenario changes, while Hubei Province is relatively less affected. This may be due to the results of the combined action of similar latitudinal intervals and domestic hydrology, or GHG emissions reach a peak or achieve a balance to a certain extent.

6. Extreme Events Analysis

Through the extreme value analysis of the temperature change prediction results, the average annual days of possible heat wave events at 12 stations under different scenarios and time periods are shown in Figure 10. It can be seen that, as far as the scenario is concerned, the number of days of heat waves under the RCP8.5 scenario is longer than that under the RCP4.5 scenario. As far as the provinces are concerned, Hunan Province has the longest average annual number of days of heat waves, followed by Hubei Province. Under the RCP4.5 scenario, the maximum heat wave days were 64.2 days in Gushi, 81.3 days in Wuhan, and 112.3 days in Yueyang. Under RCP8.5 scenario, the maximum number of heat wave days was 90.9 days in Gushi, 92.9 days in Wuhan, and 130.3 days in Yueyang. From the above results and trends, it can be seen that the number of days of heat waves is closely related to the temperature projections.

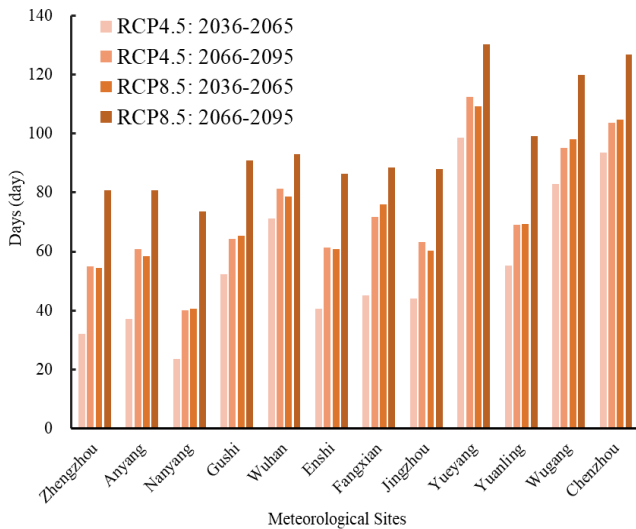


Figure 10. Average annual days of high temperature heat waves under different scenarios at each station.

In Figures 3 and 4, the temperature increasing trend of Gushi station in Henan province is obvious, while the trend of Enshi station in Hubei province is smooth. This is consistent with the probability analysis. On the whole, Hunan Province has

the largest average heat wave days, which is consistent with the temperature projections. However, there are slight differences among stations. This suggests that in addition to the effect of temperature, the latitude factor is more important for the effect of heat wave duration days.

In addition, the difference of heat wave days between stations may be related to topography and landform. For example, Wuhan and Yueyang are not the largest in temperature changes, but the days of heat wave are the longest. One reason is that their own temperature basis is high, and the circulation of urban heat island in first-tier cities will cause extreme weather such as heat wave due to the difficulty in lowering the temperature.

7. Conclusions

In summary, the future temperature in central China shows a gradually increasing trend from 2036 to 2065 and 2066 to 2095. Temperature under RCP8.5 shows a greater increase in temperature compared to the RCP4.5 scenario. The average annual duration of heat waves is 74.7 days. Details are listed as follows: (1) Future temperature in Central China shows an overall increasing trend from 2036 to 2065 and 2066 to 2095, which suggests that impacts of greenhouse gas emissions are continuous and cumulative. (2) Future temperature in Central China will increase in the future under both RCP4.5 and RCP8.5, while the increase under RCP8.5 will be greater. Among all the provinces in Central China, Hunan Province has the largest increase, followed by Hubei Province, and Henan Province is the last. This suggests that more greenhouse gas emissions will lead to a more rapid increase in temperature, and the latitude factor is one of the crucial factors in temperature variation. (3) The duration of heat waves from 2035 to 2095 is 56.9 days, 69.4 days, and 98.0 days for Henan Province, Hubei Province, and Hunan Province, respectively. This is consistent with the results of temperature increase, indicating that high temperature and latitude are important factors for heat waves.

The main innovation of this study is the development of a coupled model of stepwise regression analysis, statistical downscaling model, and extreme value analysis, i.e., SRSD model. On the one hand, this model can solve the problem of screening and predicting factors in the process of statistical downscaling. On the other hand, it makes up for the lost data in the statistical downscaling method through the SDSM model. Applying the model to the predictions of extreme heat waves provides substantial guiding significance for the disaster prevention policy of Central China. It also provides the theoretical basis for the implementation of clean production policies and the optimization of industrial structure in the region.

It is necessary to introduce and implement policies to curb greenhouse gas emissions, which can effectively help to alleviate environmental disruption and control temperature increases. In addition, as the geographical and social environment varies in different provinces, the implementation of policies should be considered in combination with local conditions to promote their development. It is also necessary to prevent extreme heat waves. Measures such as afforestation to combat soil erosion and pro-

mote water circulation, regulating reservoir storage, and industrial restructuring into cleaner production can have an effect on shortening the duration of heat waves.

In this study, there are several limitations. Due to the restricted number of GCM model and RCP scenario, comparison of the fit among multiple simulations is not allowed. In addition, the evaluation index of heat waves is relatively single, which is not sufficient enough. In the analysis of heat waves, the daily average temperature is used rather than the daily maximum temperature, which leads to fewer heat wave days compared with observed data.

Acknowledgments. This research was supported by the Fundamental Research Funds for the Central Universities, the special fund of State Key Joint Laboratory of Environment Simulation and Pollution Control, the Natural Science Foundation (U2040212, 52279002, 52279003, 52221003), the Strategic Priority Research Program of Chinese Academy of Sciences (XDA20060302).

References

- Chen, W., Jiang, Z. and Huang, Q. (2012). Projection and simulation of climate extremes over the Yangtze and Huaihe River Basins based on a Statistical Downscaling Model. *Transactions of Atmospheric Sciences*, 35(5), 578-590. <https://doi.org/10.13878/j.cnki.dqkxxb.2012.05.010> (in Chinese)
- China Meteorological Administration (2020). *Blue Book on Climate Change in China 2020*. Science Press, Beijing.
- Fan, L., Chen, D., Fu, Z. and Yan, Z. (2013). Statistical downscaling of summer temperature extremes in northern China. *Advances in Atmospheric Sciences*, 30(04), 1085-1095. <https://doi.org/10.1007/s00376-012-2057-0>
- Fu, F., Zhou, S., Pan, G., Yang, W. and Rong, T. (2003). Multiple regression analysis of maize drought tolerance coefficient. *Journal of Crops*, 29(3), 468-472. <https://doi.org/10.3321/j.issn:0496-3490.2003.03.027> (in Chinese)
- Gu, B., Xie, F., Qian, H. and Lei, L. (2019). Prediction and extreme value estimation of effective temperature of inverted Y-shaped concrete bridge tower in the lower Yangtze River. *Journal of Southeast University (Natural Science Edition)*, 49(6), 1124-1129. <https://doi.org/10.3969/j.issn.1001-0505.2019.06.015> (in Chinese)
- Guo, Y., Li, T., Cheng, Y., Ge, T., Chen, C. and Liu, F. (2012). Projection of heat-related mortality impacts under climate change scenarios in Shanghai. *Chinese Journal of Preventive Medicine*, 11, 1125-1129. <https://doi.org/10.3760/cma.j.issn.0253-9624.2012.11.014> (in Chinese)
- Liu, W., Xiong, H., Liu, L., Zhu, S. and Chen, X. (2019). Estimate of the climate change in Ganjiang River Basin using SDSM method and CMIP5. *Research of Soil and Water Conservation*, 26(2), 145-152. <https://doi.org/10.13869/j.cnki.rswc.2019.02.021>
- Shi, D. (2006). *Practical Extreme Value Statistical Method*. Tianjin Science and Technology Press, Tianjin, pp 1-30.
- National Early Warning Information Release Center. Wuhan city, Hubei Province, has issued a yellow alert for high temperatures. <http://www.cneb.gov.cn/2021/08/02/ART11627863267387217.shtml> (accessed April 1, 2022).
- Wang, H., Zhang, Z. and Tenenhaus, M. (2006). Multiple linear regression modeling method based on the compositional data. *Journal of Management Science*, 9(4), 27-32. <https://doi.org/10.3321/j.issn:1007-9807.2006.04.004> (in Chinese)
- Wilby, R.L., Hay, L.E. and Leavesley, G.H. (1999). A comparison of downscaled and raw GCM output: implications for climate change scenarios in the San Juan River basin, Colorado. *Journal of Hydrology*, 225(1-2), 67-91. [https://doi.org/10.1016/S00221694\(99\)00136-5](https://doi.org/10.1016/S00221694(99)00136-5)
- Wu, G. (2009). *Probability theory and Mathematical Statistics*. 3rd ed. China Renmin University Press.
- Wu, J. and Wang, F. (1998). A review of climate change scenario generation technology. *Meteorology*, (2), 3-8. <https://doi.org/10.7519/j.issn.1000-0526.1998.02.001> (in Chinese)
- Zheng, J., Liu, Y., Ge, Q. and Hao, Z. (2015). Spring phenodate records derived from historical documents and reconstruction on temperature change in Central China during 1850-2008. *Geographical Journal*, 70(5), 696-704. <https://doi.org/10.11821/dlxb201505002> (in Chinese)
- Zhang, X., Tang, Q. and Zhang, Y. (2021). Discussion on operational extreme value and statistical method of mohe low temperature. *Equipment Environmental Engineering*, 18(9), 125-131. <https://doi.org/10.7643/issn.1672-9242.2021.09.019> (in Chinese)